***Advances in Nanoparticles*, 2013, 2, 236-240**
http://dx.doi.org/10.4236/anp.2013.23033 Published Online August 2013 (http://www.scirp.org/journal/anp)

Isolated Cobalt Nanoparticles Prepared on HOPG in Ultrahigh Vacuum Using Thermal Annealing*

Denis Lebedev, Niyaz Nurgazizov, Anton Chuklanov, Anastas Bukharaev
Zavoisky Physical-Technical Institute (ZPhTI), Kazan, Russia
Email: denis.lebedev@bk.ru

Received March 5, 2013; revised April 5, 2013; accepted April 12, 2013

ABSTRACT

Cobalt nanoparticles on the surface of highly oriented pyrolytic graphite have been studied by atomic force microscopy. Thermal annealing in ultrahigh vacuum was used to change the size of cobalt nanoparticles and their surface distribution. The effect of two key parameters, annealing time and temperature, on the size and the surface distribution of nanoparticles has been studied. The dependence of the particle size on these parameters has been obtained. It has been shown that the main mechanism of the nanoparticle growth is Ostwald ripening.

Keywords: Nanoparticles; Thermal Annealing; Ultrahigh Vacuum; HOPG

1. Introduction

Recently, a great deal of attention was paid to developing methods of preparing nanoparticles of different metals with the given size distribution and location on the substrate surface using chemical [1-4] and physical methods [5,6]. For example, these nanoparticles are applied as catalysts for the electrochemical reactions [7]. Ferromagnetic nanoparticles can be used for the information storage devices [8,9].

Condensation methods are often used for the preparation of nanoparticles. In this case, the particles are formed on the surface as a result of the deposition of atoms from the supersaturated metal vapors. Usually the deposition is performed under high or ultrahigh vacuum conditions. Different ways of evaporation are used to create the necessary concentration of metal vapors: laser ablation [10], thermal evaporation [11], arc discharge, and evaporation in the plasma [12]. However, the use of condensation methods has some limitations associated with the control of the metal deposition conditions. In particular, it is rather difficult to prepare particles with the given shape and the narrow size distribution histogram. The size range of the produced particles and their surface distribution may be significantly expanded by the subsequent thermal annealing of samples.

The process of formation of nanoparticles on the surface conventionally can be divided into three stages [13]. The first stage is the formation of stable clusters from the deposited atoms, it may include the nucleation and spinodal decomposition. The next step in the formation of nanoparticles can be called "the early stages of growth of nanoparticles." At this stage, the clusters grow mainly due to capturing of the atoms that condensed on the surface, and also due to the diffusion of adatoms along the surface. Adatom concentration reaches the equilibrium value at the later stage growth of the particle. These processes include the Ostwald ripening and coalescence. Ostwald ripening was first observed in 1900, during the growth of mercury oxide particles in solution [14]. However, the strict formulation of a problem of the evolution of adatoms systems in the stage of Ostwald ripening, is given only in a series of papers by Lifshitz and Slezov [15], later this approach was independently developed by Wagner [16]. This model is called the Lifshitz-Slezov-Wagner theory (theory LSV).

In this work, thermal annealing in ultrahigh vacuum was used to form isolated cobalt nanoparticles and to vary their size and distribution on the highly oriented pyrolytic graphite (HOPG). It is important to note that the effect of two key parameters, annealing time and temperature, on the size and the surface distribution of nanoparticles was studied.

2. Experiment

Samples under study were HOPG plates, on the surface

*The work was supported in part by the Physical Department of the Russian Academy of Sciences.

of which nanoparticles were formed. The choice of such a substrate for the formation of particles was due to the fact that the HOPG structure is studied well, and its surface is atomically smooth terraces. The atomically smooth surface of the substrate strongly simplifies the identification of the particles on the surface and the further mathematical processing of images of nanoparticles obtained using an atomic force microscope (AFM).

Cobalt nanoparticles on the HOPG surface were formed and studied on a Multiprobe P ultrahigh vacuum (UHV) system (Omicron). This system is composed of an electron-beam evaporator (EFM 3), a scanning probe microscope (SPM) with a scan field of 9 × 9 mm, which can work in the tunnel and atomic force mode; a thermotable with the possibility of annealing samples up to the temperature of 727˚C.

A scheme of the sample preparation is shown in **Figure 1**. The substrate was a HOPG plate (size, 3 × 8 mm; thickness, 0.5 mm). The upper HOPG layer was separated with an adhesive tape immediately before loading into the UHV chamber. Then HOPG was annealed at the temperature of 727˚C for one hour to remove adsorbates from the surface and to degas the whole sample. All further operations with the sample were carried out in vacuum of better than 10^{-8} mbar.

Cobalt was deposited on the HOPG surface by evaporating the Co target (purity, 99.95%) with an electron beam having the following parameters: current emission of 40 ÷ 50 mA, accelerating voltage of 800 V, and vacuum of 6×10^{-9} mbar. The deposition time was varied in order to change the amount of cobalt deposited on the substrate. The deposition time did not exceed 10 min for all prepared samples.

We used the following technique to control the amount of material deposited on the HOPG surface. Cobalt was deposited on the substrate surface for two hours (which is substantially higher than the deposition time used to create the sample) through a mask at constant parameters of the electron-beam evaporation of the target. The mask was used to create a clear edge (step) between the region where cobalt was deposited and the region without cobalt. Then the mask was removed and the height of the resulting step was measured on an AFM which actually showed the thickness of the deposited cobalt layer. The measured height of the step was averaged taking into account roughnesses on the cobalt surface. The cobalt deposition rate was calculated on the basis on the film thickness and deposition time. It was 0.13 nm per minute.

The samples were studied in an analytical chamber using an SPM operating in the non-contact mode. In this case, the sample did not contact with the atmosphere and the size and shape distortions of nanoparticles associated with their oxidation were excluded. Ultrasharp AFM cantilevers NSG 01DLC (NT-MDT) with a whisker grown on the tip were used in the measurements. The curvature radius of the whisker apex was 1 - 3 nm that made it possible to significantly reduce the effect of the convolution on the resultant image. An example of AFM images of cobalt nanoparticles obtained with this probe is shown in **Figure 2(a)**.

It was established that cobalt nanoparticles with sizes less than 10 nm have poor adhesion to the HOPG surface, and the AFM probe working in the contact mode shifts them that makes it impossible to perform the measurements in this mode.

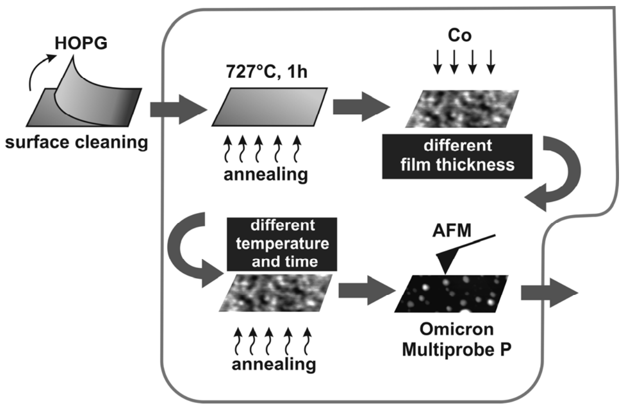

Figure 1. Stages of the formation of metal nanoparticles on the HOPG. Line outlined the stages that are implemented in ultrahigh vacuum without contact with the atmosphere.

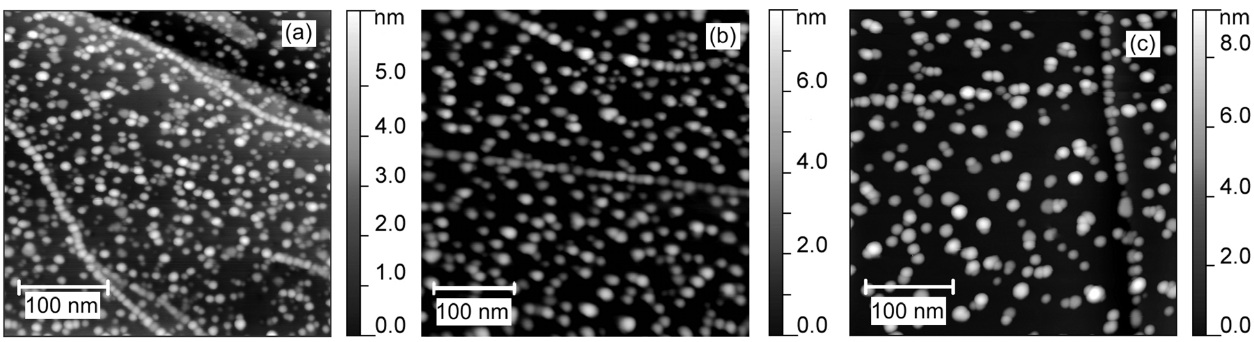

Figure 2. AFM images of Co nanoparticles on the HOPG surface obtained for the sample (a) without annealing; (b) after 30 and (c) after 200 min of thermal annealing at *T* = 450˚C.

Since the shape of produced nanoparticles may differ from the spherical one, we used two main parameters for their characterization: the particle height and its apparent radius in the sample plane. It is known that the measured height is the most reliable size parameter for isolated particles in atomic force microscopy. However, the particle radius is one of key parameters in theories of nucleation and growth, therefore its value was important for the further interpretation of the obtained results. In order to estimate the error in the determination of the lateral sizes of the particles due to the convolution effect of the probe and surface profiles, we used the deconvolution method described in [17]. In our case, the use of probes with whiskers gave an error of 5% - 10%. Therefore we used the values of the apparent radius measured from the experimental AFM images directly.

The statistical analysis of the AFM images of particles was carried out using the original computer program elaborated earlier, which makes it possible to calculate the geometric parameters of closely spaced/agglomerated particles on the surface with large-scale irregularities [18]. This program is used to calculate the radius and height of the particles. Histograms of the particle height and radius distributions, as well as graphs of the particle average height and radius as functions of annealing time and temperature were plotted after processing.

3. Results and Discussion

3.1. Effect of the Annealing Temperature on the Sizes of Co Nanoparticles

The following experiment was performed to study the dependence of the size of nanoparticles and their surface distribution on the thermal annealing temperature. The cobalt film was deposited for 3 min on the prepared HOPG surface. The amount of the material was equivalent to a continuous cobalt film with the thickness of 0.4 nm. Thermal annealing was performed consequently at different temperatures (550˚C, 650˚C, and 750˚C).

The interval of temperatures in this case was chosen by analysis of literary data [19,20]. In order to eliminate the error associated with the time of heating of the sample, the annealing time was one hour in all cases. The sample surface was studied on the AFM without contact with the atmosphere after each thermal annealing.

According to the AFM images (**Figure 3**), the average size of nanoparticles increases and their density decreases with increasing annealing temperature. On the basis of the statistical analysis results for the AFM images (**Figure 4**), the average height of the particles increases from 3.3 to 5.4 nm with the mean radius varying from 7.2 to 10.4 nm with increasing annealing temperature. The density of the particles decreases from 21×10^4 to 6×10^4 mkm^{-2}.

3.2. Effect of the Annealing Time on the Sizes of Co Nanoparticles

The following experiment was performed to study the effect of the annealing time on the sizes and the surface distribution of nanoparticles. Using the technique described above, cobalt was deposited on the HOPG surface for 30 s. The amount of the deposited material was equivalent to a continuous cobalt film with the thickness of 0.1 nm. According to the AFM results, nanoparticles were formed on the HOPG surface (**Figure 2**) with an average height of 1.4 nm and an average radius of 5.3 nm (**Figures 5(b)** and **(c)**). The density of the nanoparticles was 54×10^4 mkm^{-2} (**Figure 5(d)**).

Then the sample was consecutively annealed at the temperature of 470˚C during 15, 30, 45, 75, 135, 200, and 500 min. The heating of the sample up to 470˚C took about 1 - 2 minutes therefore the minimum interval of annealing time was chosen to be 15 minutes. The AFM measurement of the sample was performed after each thermal annealing. **Figures 2(b)** and **(c)** show typical AFM images of the sample obtained after 30 and 200 min of annealing, respectively. Histograms of the particle size (particle height and radius) were plotted for all images. **Figure 5(a)** shows histograms for the images shown

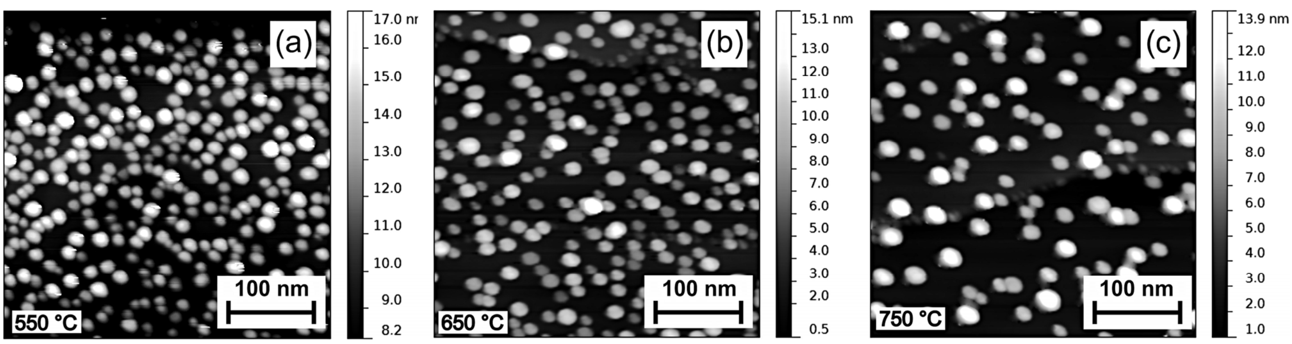

Figure 3. AFM images of Co nanoparticles on the HOPG surface obtained after thermal annealing at different temperatures: (a) 550˚C; (b) 650˚C; (c) 750˚C.

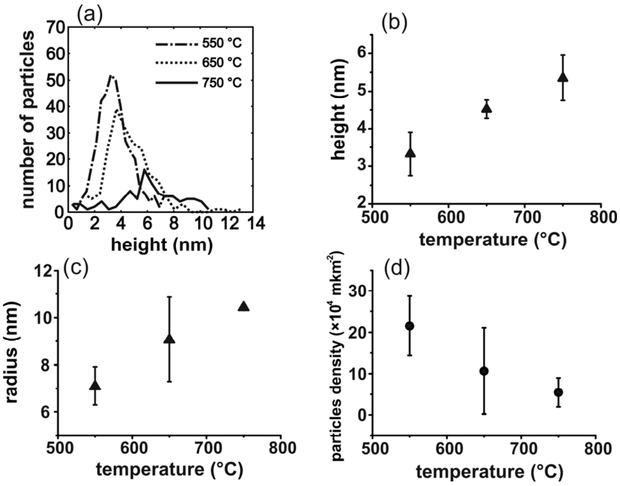

Figure 4. (a) Histograms of the height distribution of Co particles for different annealing temperatures, (b)-(d) dependences of the height, diameter and density of the particles on the annealing temperature, respectively.

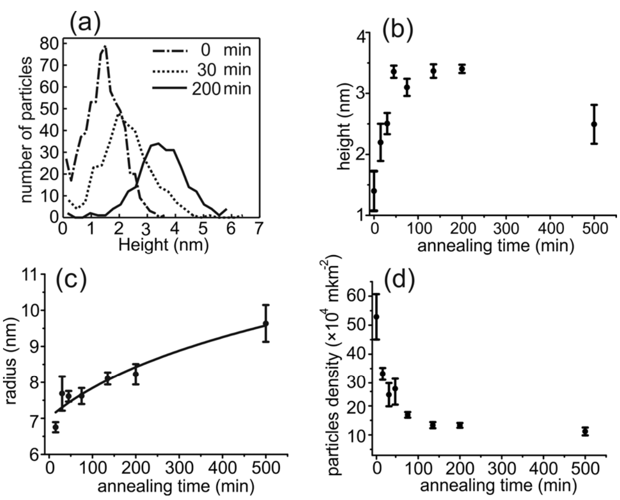

Figure 5. (a) Histograms of the height distribution of Co particles for different annealing times; annealing time dependences of: (b) the average particle height; (c) the average particle radius (solid line shows the result of the approximation by Equation (2)); (d) the density of particles per 10^4 mkm^{-2}.

in **Figure 2**. The dependence of the average sizes of the cobalt particle on the annealing time is shown in **Figures 4(b)** and **(c)**.

The particle radius increases monotonically. The particle height increases during the first hour of annealing, and then this parameter remains constant for three-four hours. After six hours, the particle height gradually decreases. The particle density decreases with time. All these facts make it possible to assume that the atoms diffuse from the surface of small particles to that of larger particles. As a result, the number of small particles decreases, and the size of the large particles increases.

This mechanism of the growth of nanoparticles corresponds to Ostwald ripening. It was theoretically described by Lifshitz and Slezov in [15]. It is known [21,22] that the following conditions are necessary for Ostwald ripening to occur:

$$\left[\pi(R+\lambda)^2\right]^{-1} < N < (\pi R^2)^{-1} \quad (1)$$

where R is the average particle radius, λ is the mean free path of atoms on the substrate, N is two-dimensional particle density. According to our estimates, this inequality is satisfied for our samples. This makes it possible to use the theory of Ostwald ripening of the nanoparticles [21] for describing our results.

In the theoretical model [21], the average particle radius depends on the annealing time as follows:

$$R(t) = \left(R_0^p + At\right)^{1/p} \quad (2)$$

where R is the average particle radius, R_0 is the average radius at the initial time, A is the constant determined by the mechanism of the mass transfer at the current temperature, p is the coefficient depending on the shape of the particles and the mechanism of the mass transfer and its value is 2, 3 or 4.

In the case of the three-dimensional growth of nanoparticles on the two-dimensional surface, the coefficient p = 4 as a result of the redistribution of the material between particles [21]. After approximating the experimental time dependence of the mean particle radius ($R(t)$) (**Figure 5(c)**) by Equation (2), the following parameter values were obtained: A = 0.251 nm^4/s; R_0 = 6.843 s. It should be noted that the calculated R_0 value is in rather good agreement with the experimental value (R_{0exp} = 5.3 ± 2.4 nm).

Thus, the nanoparticles of the given size can be produced by selecting optimum annealing time values using Equation (2) and the A value at the current temperature.

4. Conclusion

The evolution of the size and distribution of Co nanoparticles on the HOPG surface in ultrahigh vacuum depending on the annealing time and temperature was studied using AFM. It was shown that the size of nanoparticles and their surface distribution can be controlled by varying these parameters. The value of the parameter, which characterizes the mass transfer, was found assuming that the main mechanism of the particle size variation is Ostwald ripening. The parameter value makes it possible to predict the average size of cobalt nanoparticles formed on the HOPG surface as a function of the initial particle size, annealing time and temperature.

REFERENCES

[1] P. Shen, N. Chi, K.-Y. Chan, *et al*., "Platinum Nanoparti-

cles Spontaneously Formed on HOPG," *Applied Surface Science*, Vol. 172, No. 1-2, 2001, pp. 159-166. doi:10.1016/S0169-4332(00)00848-5

[2] L. Tamašauskaitė, R. Tarozaitė and A. Vaškelis, "Electrocatalytic Properties of Gold Nanoparticles in Oxidation Reactions of Reducing Agents," *Chemija*, Vol. 17, No. 4, 2006, pp. 13-19.

[3] L.P. Bicelli, B. Bozzini, C. Mele and L. D'Urzo, "A Review of Nanostructural Aspects of Metal Electrodeposition," *International Journal of Electrochemical Science*, Vol. 3, No. 4, 2008, pp. 356-408.

[4] Z. Tang, S. Liu, S. Dong and E. Wang, "Electrochemical Synthesis of Ag Nanoparticles on Functional Carbon Surfaces," *Journal of Electroanalytical Chemistry*, Vol. 502, No. 1-2, 2001, pp. 146-151. doi:10.1016/S0022-0728(01)00344-8

[5] R. G. Song, M. Yamaguchi, O. Nishimura, *et al*., "Investigation of Metal Nanoparticles Produced by Laser Ablation and Their Catalytic Activity," *Applied Surface Science*, Vol. 253, No. 6, 2007, pp. 3093-3097. doi:10.1016/j.apsusc.2006.06.059

[6] B.-X. Chung and C.-P. Liu, "Synthesis of Cobalt Nanoparticles by DC Magnetron Sputtering and the Effects of Electron Bombardment," *Materials Letters*, Vol. 58, No. 9, 2004, pp. 1437-1440. doi:10.1016/j.matlet.2003.06.018

[7] F. W. Campbell and R. G. Compton, "The Use of Nanoparticles in Electroanalysis: An Updated Review," *Analytical and Bioanalytical Chemistry*, Vol. 396, No. 1, 2010, pp. 241-259. doi:10.1007/s00216-009-3063-7

[8] Y. Inaba H. Nakata and D. Inoue, "New High Density Recording Technology: Energy Assisted Recording Media," *Fuji Electric Review*, Vol. 57, No. 2, 2011, pp. 42-45.

[9] K. Şendur and W. Challener, "Patterned Medium for Heat Assisted Magnetic Recording," *Applied Physics Letters*, Vol. 94, No. 3, 2009, Article ID: 032503.

[10] S. Noel, J. Hermann and T. Itina "Investigation of Nanoparticle Generation during Femtosecond Laser Ablation of Metals," *Applied Surface Science*, Vol. 253, No. 15, 2007, pp. 6310-6315. doi:10.1016/j.apsusc.2007.01.081

[11] S.A. Nepijko, D. Kutnyakhov, *et al*., "Structure and Magnetic Properties of One-Dimensional Chains of Ferromagnetic Nanoparticles," *Applied Physics A*, Vol. 109, No. 3, 2012, pp. 699-702. doi:10.1007/s00339-012-7103-3

[12] F. Fendrych, L. Kraus, O. Chayka, *et al*., "Preparation of Nanostructured Magnetic Films by the Plasma Jet Technique," *Monatshefte Fur Chemie*, Vol. 133, No. 6, 2002, pp. 773-784. doi:10.1007/s007060200049

[13] M. Zinke-Allmang, L. C. Feldman and M. H. Grabow, "Clustering on Surfaces," *Surface Science Reports*, Vol. 16, No. 8, 1992, pp. 377-463. doi:10.1016/0167-5729(92)90006-W

[14] W. Ostwald, "On the Supposed Isomerism of Red and Yellow Mercury Oxide and the Surface Tension of Solid Bodies," *Journal of Physical Chemistry B*, Vol. 34, 1900, p. 495.

[15] I. M. Lifshitz and V. V. Slyozov, "The Kinetics of Precipitation from Supersaturated Solid Solutions," *Journal of Physics and Chemistry of Solids*, Vol. 19, No. 1-2, 1961, pp. 35-50. doi:10.1016/0022-3697(61)90054-3

[16] C. Wagner, "Theorie der Alterung von Niederschlagen durch Umlösen (Ostwald-Reifung)," *Z. Elektrochem*, Vol. 65, No. 7-8, 1961, p. 581-591.

[17] A. A. Bukharaev, N. V. Berdunov, D. V. Ovchinnikov, *et al*., "Atomic Force Microscopy for Metrology of Micro- and Nanostructures," *Russian Microelectronics*, Vol. 26, No. 3, 1997, pp. 137-148.

[18] A. P. Chuklanov, A. A. Bukharaev and S. A. Ziganshina, "Computer Program for the Grain Analysis of AFM Images of Nanoparticles Placed on a Rough Surface," *Surface and Interface Analysis*, Vol. 38, No. 4, 2006, pp. 679-681. doi:10.1002/sia.2294

[19] I. Beszeda, E. G. Gontier-moya and A. W. Imre, "Surface Ostwald-Ripening and Evaporation of Gold Beaded Films on Sapphire," *Applied Physics A*, Vol. 81, No. 4, 2005, pp. 673-677. doi:10.1007/s00339-005-3254-9

[20] F. Fillot, Zs. Toke and G. P. Beyer, "Surface Diffusion of Copper on Tantalum Substrates by Ostwald Ripening," *Surface Science*, Vol. 601, No. 4, 2007, pp. 986-993. doi:10.1016/j.susc.2006.11.037

[21] S. A. Kukushkin and A. V. Osipov, "New Phase Formation on Solid Surfaces and Thin Film Condensation," *Progress in Surface Science*, Vol. 151, No. 1, 1996, pp. 1-107. doi:10.1016/0079-6816(96)82931-5

[22] S. A. Kukushkin and A. V. Osipov, "Thin-Film Condensation Processes," *Physics Uspekhi*, Vol. 41, No. 10, 1998, pp. 983-1014. doi:10.1070/PU1998v041n10ABEH000461

